

Subproject C4.9

Electrochemistry with an electron beam – local metal deposition in ionic-liquid and molten-salt thin films

Principle Investigators: Rolf Schuster

CFN-Financed Scientists: Vadym Halka(BAT IIa, 18 months)

Further Scientists: Vasevolod Avrutskiy, Matthias J. Schmid

**Institut für Physikalische Chemie
Universität Karlsruhe (TH)**

Electrochemistry with an electron beam – local metal deposition in ionic-liquid and molten-salt films

Introduction and Summary

Functional properties of metallic micro- and nanostructures are very sensitive on their size and shape. Designing their functionally therefore requires techniques for their fabrication. Lithographical processes are among the most important techniques in this respect. However, metallic structures like chip interconnects are mostly obtained by a sequential process where e.g., first a polymer mask is lithographically patterned and subsequently coated with metal [1]. In this project, we use a focused electron beam for the direct, local reduction of metal ions in thin electrolyte films of molten AgNO_3 or a metal salt solution in an ionic liquid (IL). This allows direct electron irradiation of the electrolyte film in vacuum, due to the low vapour pressure of the molten salts.

Using a liquid electrolyte film as precursor for the metal deposition instead of gaseous or solid ones [2-4] has several advantages: i) Charging of the surface is effectively avoided due to the ionic conductivity. Hence, also nonconductive substrates like glass can be directly coated with metal patterns. ii) Effective mass transport in the liquid film allows for the deposition of μm -thick structures. iii) Precipitation of reduced metal from the film onto the surface proceeds via nucleation and growth. Therefore, the morphology of the deposits is strongly dependent on the irradiation parameters. We deposited metallic structures, ranging from patterns of Ag nanocrystallites up to thick, conductive Ag lines. First attempts to quantitatively model the deposition process are in progress.

While deposition of Ag from a molten AgNO_3 films was rather thoroughly investigated (a publication is submitted [C4.9:1] [5]), the use of IL based electrolytes has still to be explored. The use of IL is hampered by the polymerization of the liquid film upon electron irradiation. We try to circumvent this problem by the use of low energy electrons for the irradiation. First test experiments were conducted successfully. A small vacuum chamber, equipped with a low energy electron gun was set up. The groups of C. Feldmann and P. W. Roesky provide support for choosing the IL and corresponding metal salts. Beside characterization of the deposition process future work will concentrate also on properties of the produced particle patterns. Examples are measuring cathodoluminescence or optical excitation of plasmons in particle patterns and studies of cell adhesion on custom made patterns.

1. Direct reduction of metal ions by free electrons

Conducting metal reduction with free electrons is in principle an old approach. In 1887 Gubkin [6] deposited Ag-colloids at the surface of an aqueous AgNO_3 electrolyte by electrons, produced in a gas discharge in the partly evacuated gas volume above the liquid surface. The anode was formed by the electrolyte surface itself. As demonstrated recently, e.g., by Janek and coworkers, the emergence of ionic liquids, i.e., room temperature molten salts with a negligible vapor pressure, allows for well defined control of the discharge parameters and the deposition of colloidal Ag in the electrolyte solution [7, 8]. We extended this approach to the irradiation of μm -thin electrolyte films on a substrate.

It is straight forward to use the electron beam of a SEM for irradiating the electrolyte film. In first experiments we irradiated a spin coated film of $\text{CF}_3\text{SO}_3\text{Ag}$ in $[\text{BMIm}][\text{TfO}]$. The result after washing off the ionic liquid is shown in fig. 1a). In the irradiated area the IL polymerized and the film appeared slightly opaque in the light microscope. This indicates the inclusion of small particles, very probably small Ag particles, immobilized in the polymer. Unfortunately we were not able to remove the polymer without washing off the inclusions. Although interesting in its own, we aimed at the deposition of metal particles without polymer matrix. We approached this objective via two routes, firstly by employing a molten film of AgNO_3 at 260°C which was not susceptible to polymerization in the SEM and secondly by irradiation of an ionic liquid film with low energy electrons, in order to avoid radiation chemistry and polymerization of the ionic liquid.

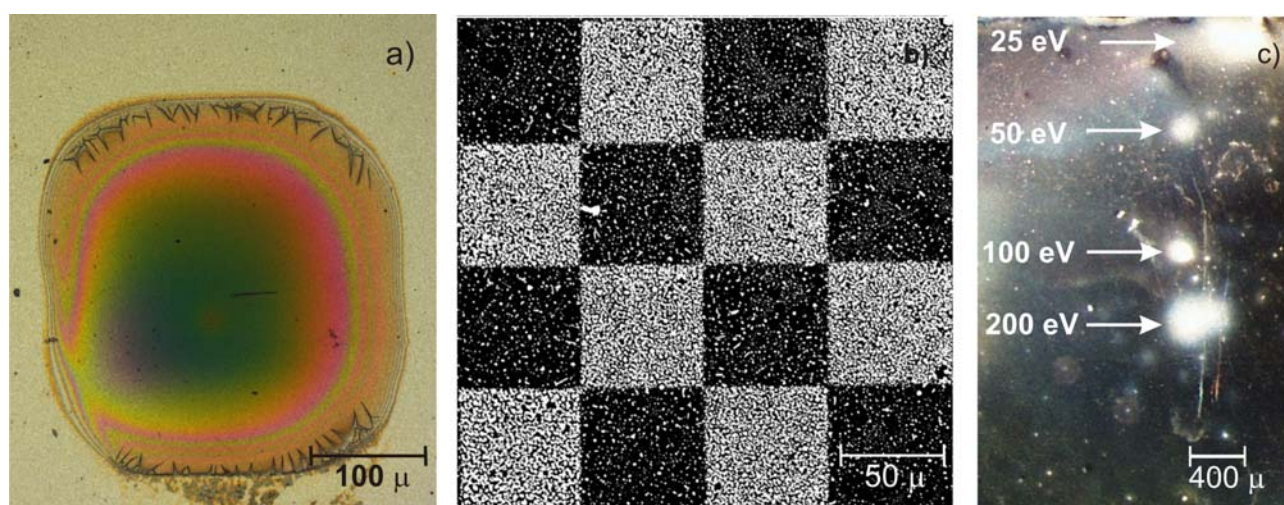


Figure 1: (a) polymerized IL film with particle inclusions on glass, obtained from irradiation of $\text{CF}_3\text{SO}_3\text{Ag}$ in $[\text{BMIm}][\text{TfO}]$ by 15 keV electrons. (b) Check board pattern of Ag nanoparticles obtained by irradiation of a molten AgNO_3 film in the SEM. (c) Ag deposited on glass from $\text{CF}_3\text{SO}_3\text{Ag}$ in $[\text{BMIm}][\text{TfO}]$ by a slightly focussed low energy electron beam.

In principle, both routes were successful. Figure 1b shows a check board pattern of Ag nanocrystallites, deposited from AgNO_3 in an SEM with a focused 15 keV electron beam. For this system we studied the dependence of particle size and density on the irradiation parameters in detail, which allowed deriving conclusions on the deposition mechanism. Cathodoluminescence measurements for characterizing the optical properties were also conducted in collaboration with subproject C4.8. For the second route, i.e., low energy electron irradiation of IL, first test experiments were performed. Since focusing of low energy electrons is subtle, we employed a commercial electron gun, with beam energies down to 10 eV and a focal diameter of about 0.5 mm. The results of low energy irradiations are shown in fig. 1c. Polymerization of the IL could be avoided due to the low electron energy and the IL was completely washed off after irradiation.

2. Ag deposition from molten AgNO_3 films

Due to the ionic conductivity of the electrolyte film, the deposition of metallic patterns is possible on conductive and non-conductive substrates. Figure 2 shows checkboard patterns of Ag nanoparticles deposited onto silicon, Ta and glass by irradiation of an about 1-3 μm thick molten

AgNO₃ film at 260°C with a 15keV focused electron beam in a SEM. The bright areas of the checkboards were repetitively scanned with about 1 nA beam current, a scan speed of 1 mm/s and 500 lines per bright patch. Along the trace of the e-beam Ag nanoparticles grew, which strongly stuck to the surface so that the salt film could be washed off after the irradiation, with the metal structures remaining on the surface. Closer inspection of the irradiated areas reveals that rather regularly shaped crystallites formed on the surface with a broad size distribution ranging from a few 100 nm up to more than 1 μm. Using a thin liquid electrolyte film was crucial for the success of the patterning process: Although after irradiation of a solid AgNO₃ film the irradiated areas appear greyish in the light microscope, after washing off the salt film, no structures remained on the surface. Also melting of the salt film for about 10 min at 260 °C, directly following e-beam irradiation of the solid film, did not lead to the formation of patterns, which reside on the surface.

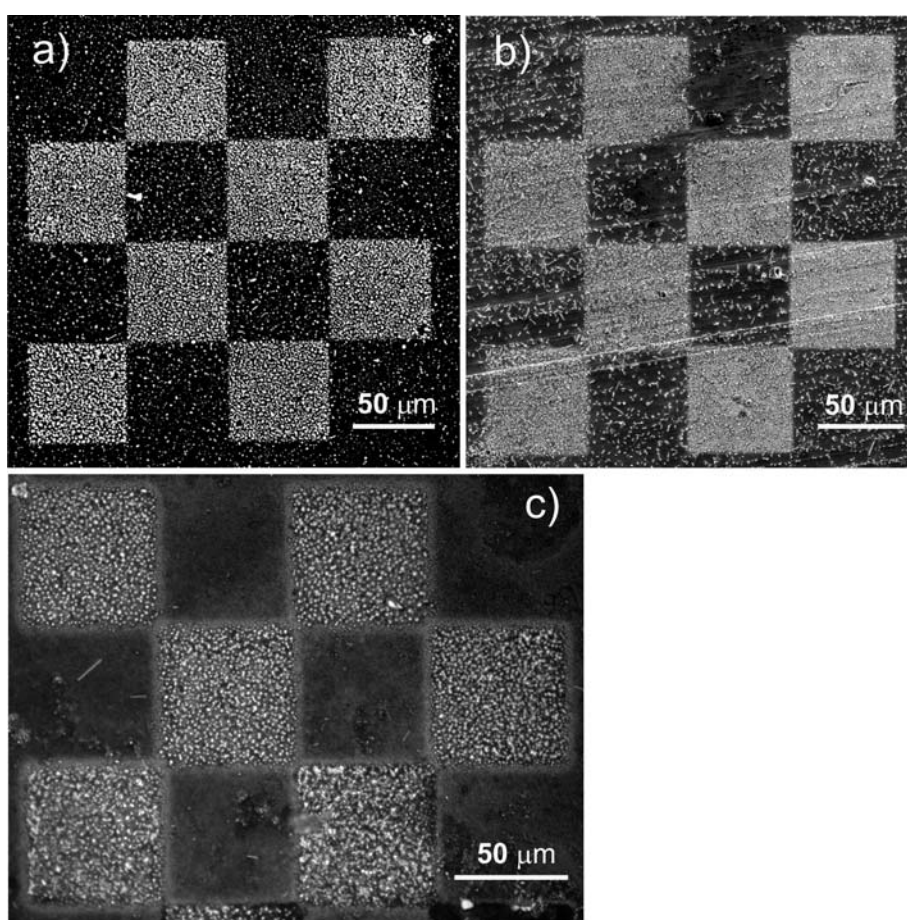


Figure 2: Checkboard patterns of Ag particles on Si (a), Ta (b) and glass (c), formed by irradiation of a 1 – 3 μm thick liquid AgNO₃ film at 260°C with a 15 keV electron beam in an SEM. The figures show SEM images (a,b) and an optical micrograph (c) of the surfaces after washing off the salt film.

The irradiation parameters like scan speed, beam current and irradiation time had pronounced influence on the observed structures. Figure 3a and 3b present details of nanoparticle patterns on Si, which were obtained with the same total dose of 1.8 mC/cm² and the same beam current (0.3 nA), but with scan speeds, differing by almost three orders of magnitude, and correspondingly different

repetition times. Visual inspection already reveals that with faster scan speed larger particles were obtained, however, with a lower number density. Statistical analysis resulted in average radii of 250 nm and 420 nm for the fast and slow scan, respectively. Within experimental errors the deposited amount of Ag is about the same for both figures with a total yield of ca. 50 Ag atoms per primary electron. Similarly also the electron dose, deposited in the film strongly influenced the particle size and shape. Figure 3c was obtained after irradiation with a 7-fold dose, compared with fig. 3a and b. The particle size increased considerably and most of the particles exhibit well developed crystal facets. Smaller particles disappeared almost completely and the density of particles strongly decreased. However, the total Ag yield remained about the same as with lower dose. It should be noted that the coarsening of the patterns upon increasing the electron dose cannot be attributed to a simple Ostwald mechanism, since the ripening process is independent of the annealing time and only proceeds during electron irradiation.

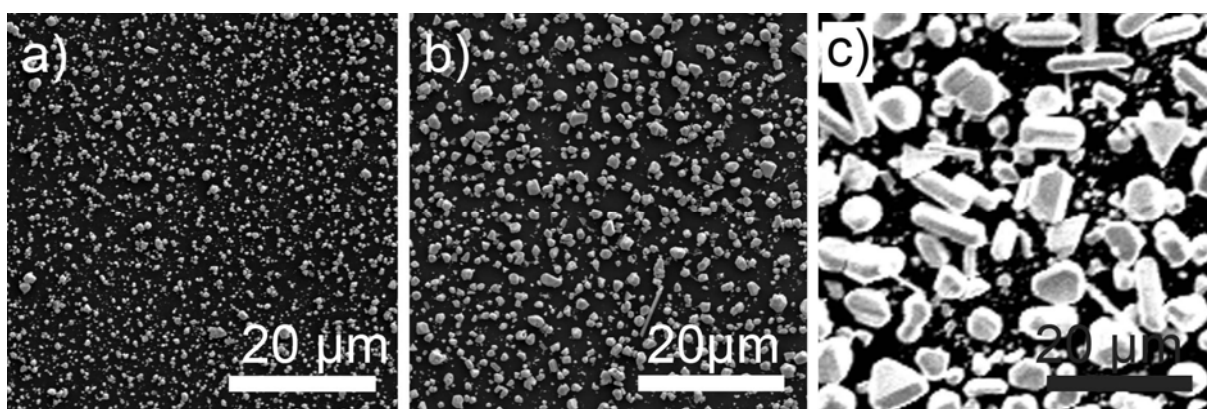


Figure 3: SEM images of Ag deposits on Si, obtained with varying irradiation parameters. (a) and (b) were deposited with the same dose of 1.8 mC/cm^2 and the same beam current of 0.3 nA, but with differing scan rates of 2 mm/s (a) and 1000 mm/s (b). The repetition times were 10 ms and 2.5 s. In (c) the total dose was 12 mC/cm^2 obtained with a scan rate of 500 mm/s and a beam current of 1 nA.

The high yield for the Ag deposition points to a radiation chemical reaction, whereby Ag ions in the electrolyte are reduced upon decomposition of the AgNO_3 and concomitant evolution of gaseous reaction products. This was substantiated by measurements of the sample current upon varying bias voltage, which indicated no significant amount of charged reaction products leaving the sample. The primary radiation chemical process will probably form finely dispersed Ag atoms in the film, which will tend to agglomerate into larger particles similar to the formation of Ag colloids upon electron irradiation of ionic liquids [7, 8]. The strong dependence of the particle density on the scan speed is a direct consequence of the nucleation process during particle formation. Upon slow scanning, a higher local Ag concentration built up in the beam spot than during fast scanning, leading to a higher nucleation rate and therefore to more nuclei, i.e., higher Ag particle density. Repetition of the pattern on a timescale of 10 ms, as employed for the fast scan in fig. 3b, could not compensate for the short residing time per point. With increasing irradiation time, i.e., total dose, the Ag particles further grew and developed pronounced facets (fig. 3c). This deposit was formed with a scan speed of 500 mm/s, a beam current of 1 nA and a total dose 12 mC/cm^2 , which is about 7 times higher than that of the patterns in fig. 3a and b. First simulations of the deposition process are in preparation.

3. Metal deposition with low energy electrons

Low energy electrons were employed for the deposition of Ag from both, molten AgNO_3 films and films of metal salt solutions in IL. For first test experiments, when no commercial low energy electron gun was available, electrons emitted from a tungsten filament were accelerated by application of about 7 to 10 V to a pinhole of about 1 mm diameter, in close proximity of the electrolyte-coated substrate surface. Ag could be deposited from IL films in these test experiments, however, the deposition parameters were badly controlled and the deposits were fairly irregular. Figure 4 shows Ag deposits on Au from $\text{CF}_3\text{SO}_3\text{Ag}$ in $[\text{BMIm}][\text{TfO}]$ (fig. 4a) as well as Al deposited from $\text{AlCl}_3 / \text{MBIC}$ mixtures (fig. 4b).

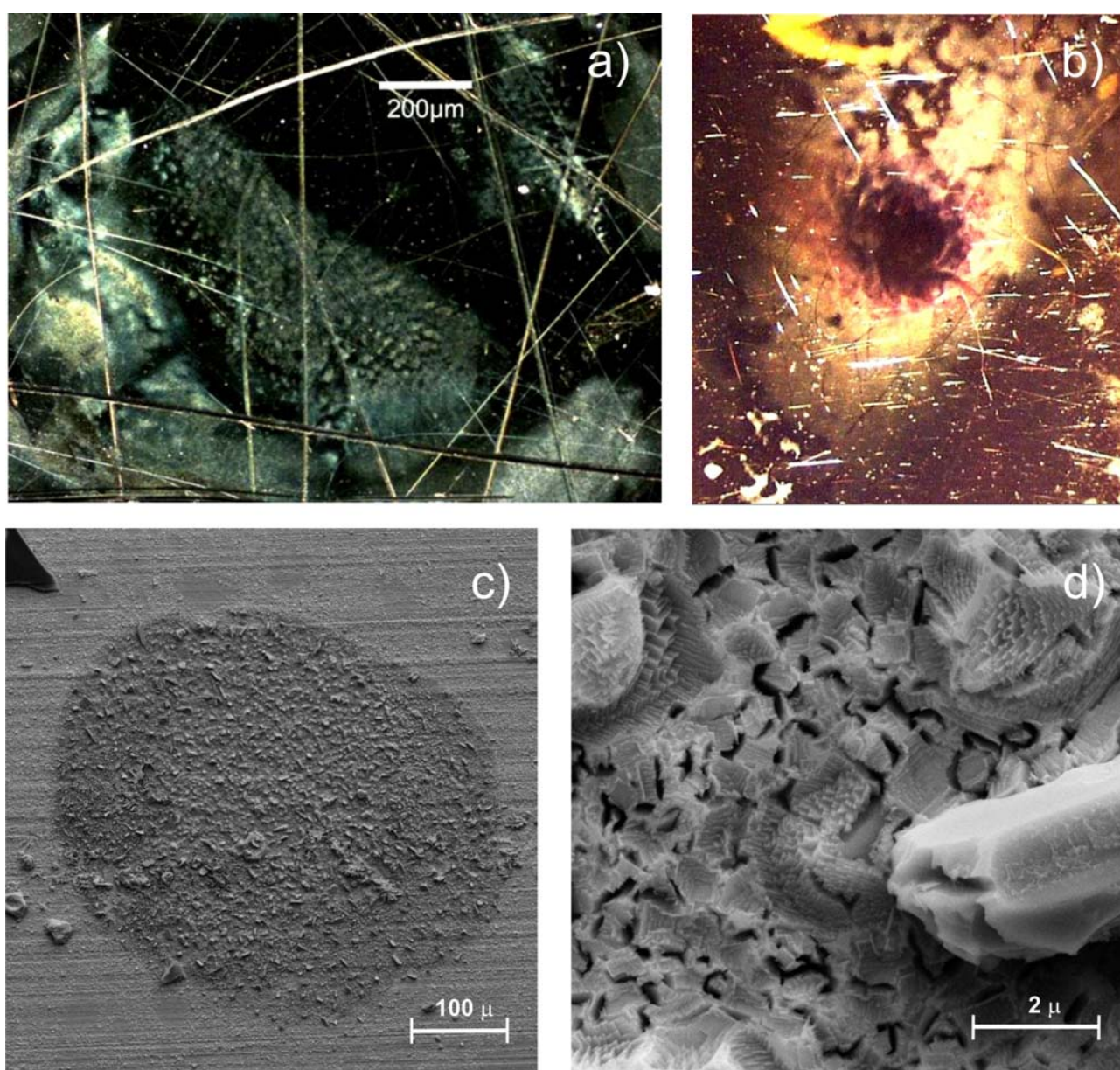


Figure 4:(a) Ag deposition by 7 eV electrons from $\text{CF}_3\text{SO}_3\text{Ag}$ in $[\text{BMIm}][\text{TfO}]$. (b) Al deposited with 7 eV from $\text{AlCl}_3 / \text{MBIC}$ mixtures. (c) Ag Spot obtained with a weakly focused 2 keV

electron beam on molten AgNO_3 on Ta. (d) Detail of fig.4c, showing small faceted Ag crystallites forming a homogeneous dense layer with additional large Ag crystallites.

In order to improve the control of the irradiation parameters, we built a small vacuum chamber with a commercial electron gun (Kimball Physics Inc.), which supplied electrons with energies between 5 and 2000 eV and beam currents up to 20 μA (at higher energies). The electron beam can be slightly focused to an about 0.5 mm diameter beam spot. Figure 1c shows optical micrographs of four silver dots, obtained at beam energies between 25 eV and 200 eV with the new electron gun. Similarly to the deposition from molten AgNO_3 at high beam energies, the deposits consisted of Ag microcrystallites, which were strongly attached to the substrate so that the IL could be washed off after the experiment. The deposits were obtained with about 200 nA beam current and 30 min irradiation time.

It should be noted at this point that the deposition process with low energy electrons is distinctively different from the processes with high energy electrons in the SEM. Due to the low electron energy, significant radiation chemical processes can be excluded and the formation process of elementary silver must become essentially an electrochemical reduction of Ag ions by incoming electrons. It is unclear, whether the electrons effectively solvate and thermalize before reduction of silver occurs. However, from spectroscopic experiments a significant lifetime of up to several 100 ns was found for solvated electrons produced by light pulses in IL in the absence of electron scavengers [9]. Although quantitative information is not available at the present stage of the experiments, we expect the yield for silver reduction and deposition to be close to one. The reduction process should be similar to the formation of Ag colloids in bulk Ag/IL solutions by electrons from a glow discharge [7, 8], where the electrons reaching the liquid surface have probably an energy far below 100 eV.

The influence of the beam energy on the morphology of the deposits is demonstrated in figs. 4c and 4d where Ag was deposited from molten AgNO_3 by 2 keV. In contrast to the irradiation in the SEM with 15 keV electrons (see fig. 3) mostly cubic crystallites were formed, which were interconnected and formed a rather homogeneous layer with a thickness of a few 100 nm. Clear faceting indicated slow growth of the crystallites. It should be noted that sporadically large crystallites evolved on top of the homogeneous layer, which stuck several microns above the surface (see fig. 4d, lower right).

4. Optical Properties

In the beginning of the project the formation of patterns of rather finely dispersed Ag particles under suitable irradiation conditions was rather surprising. However, the fabrication of well defined particle arrays is usually rather difficult and our method might open new avenues for the straight forwards generation of nanoparticle patterns.

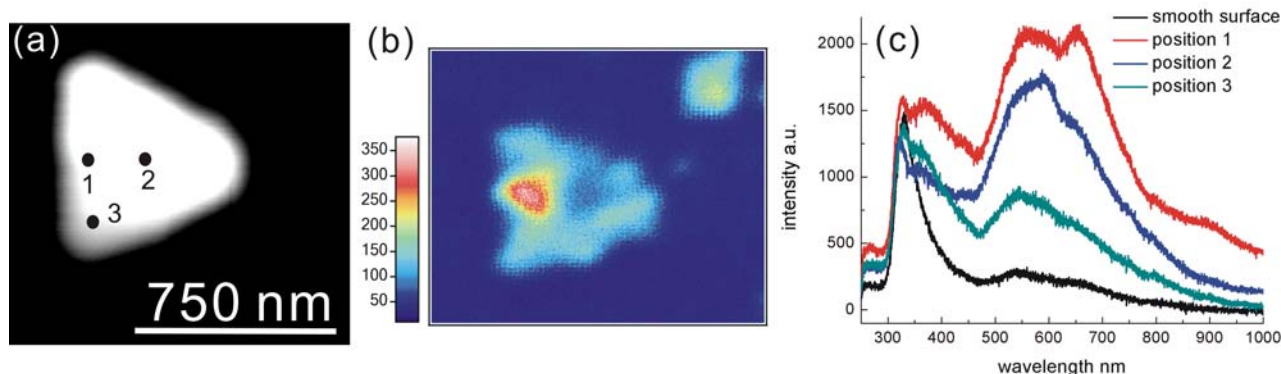


Figure 5: (a) SEM image of a triangular Ag nanoparticle on a Si substrate. (b) Photon map of the Ag particle in (a) upon 15keV electron irradiation (integration time: 5 ms/pixel). (c) Cathodoluminescence spectra obtained upon irradiation at three different position at the particle in (a) (beam current: 3 nA , integration time: 50s). In addition a cathodoluminescence spectrum of a clean Ag surface is shown.

As a first step towards the characterization of the properties of the deposited particle patterns, we investigated their cathodoluminescence upon electron irradiation in collaboration with project C4.8. Figure 5 shows cathodoluminescence data of a single Ag particle on Si, which was created by 15 keV electron irradiation of molten AgNO_3 under the conditions of fig. 3b. The data were obtained in a scanning electron microscope, which was equipped with a parabolic mirror for the detection of light emitted from the sample. The light was either focussed on the cathode of a photomultiplier with sensitivity between 300 nm and 850 nm or onto the slit of a spectrometer, equipped with a cooled CCD camera as detector. As can be seen in the panchromatic photon map of the particle upon electron irradiation rather strong emission of light was observed, when the electron beam hit the particle (fig. 5b). The electron induced light emission was not homogeneously distributed across the particle. Indeed the photon map exhibited more structural details than the simultaneously recorded secondary electron image of the particle. The strongest emission was about two times higher than that of the rest of the particle. Spectra upon electron irradiation of different locations of the particle can be seen in fig. 5c. In addition the spectrum of a flat Ag surface is shown, which exhibits a peak at about 330 nm, originating from deexcitation of Ag bulk plasmons [10]. Similarly at the Ag particle emission peaks were found at about 330 nm. Additional spectral features indicate emission from localized plasmon modes of the particle. Strong variations of the emitted light intensity can be seen for irradiation of different locations with the strongest intensity found in position 1, which is in accordance with the panchromatic image in fig. 5b. At a wavelength between 450 nm and about 800 nm strong variations of both, the spectral shape and the overall intensity were observed. In particular irradiation of position 1 resulted in an peak at 660 nm, which was less strongly excited at the other beam positions.

References

- own work with complete titles -

- [1] P. Rai-Choudhury ed., *Handbook of Microlithography, Micromachining, & Microfabrication* (SPIE Optical Engineering Press, Bellingham, WA, 1997).
- [2] T. Lukaszcyk, M. Schirmer, H.-P. Steinrück, and H. Marbach, *Small* **4**, 841 (2008).
- [3] J.-O. Malm, G. Schmid, and B. Morun, *Phil. Mag. A* **63**, 487 (1991).

- [4] Y.-H. Pai, H.-F. Huang, Y.-C. Chang, C.-C. Chou, and F.-S. Shieu, *J. Power Sources* **159**, 878 (2006).
- [5] V. Halka, M. Schmid, V. Avrutskiy, and R. Schuster, *Electron beam induced deposition of metallic microstructures from a molten salt film on conductive and nonconductive substrates*, submitted (2010).
- [6] J. Gubkin, *Ann. Phys. Chem. N. F.* **32**, 114 (1887).
- [7] A. Imanishi, M. Tamura, and S. Kuwabata, *Chem. Commun.*, 1775 (2009).
- [8] S. A. Meiss, M. Rohnke, L. Kienle, S. Z. E. Abedin, F. Endres, and J. Janek, *ChemPhysChem* **8**, 50 (2007).
- [9] C. Nese and A.-N.-. Unterreiner, *Phys. Chem. Chem. Phys.* **12**, 1698 (2010).
- [10] P. Chaturvedi, K. H. Hsu, A. Kumar, K. H. Fung, J. C. Mabon, and N. X. Fang, *ACSNano* **3**, 2965 (2009).